HHS Public Access

Author manuscript

Sci Signal. Author manuscript; available in PMC 2017 August 28.

Published in final edited form as:

Sci Signal. ; 6(274): ra31. doi:10.1126/scisignal.2003705.

Phenobarbital indirectly activates the constitutive active androstane receptor (CAR) by inhibition of epidermal growth factor receptor signaling

Shingo Mutoh[1], **Mack Sobhany**[1], **Rick Moore**[1], **Lalith Perera**[2], **Lee Pedersen**[2], **Tatsuya Sueyoshi**[1], and **Masahiko Negishi**[1,*]

[1]Pharmacogenetics Section, Laboratory of Reproductive and Developmental Toxicology, National Institute of Environmental Health Sciences, National Institutes of Health, Research Triangle Park, North Carolina 27709, USA

[2]Laboratory of Structural Biology, National Institute of Environmental Health Sciences, National Institutes of Health, Research Triangle Park, North Carolina 27709, USA

Abstract

Phenobarbital is a central nervous system depressant that also indirectly activates nuclear receptor constitutive active androstane receptor (CAR), which promotes drug and energy metabolism, as well as cell growth (and death), in the liver. We found that phenobarbital activated CAR by inhibiting epidermal growth factor receptor (EGFR) signaling. Phenobarbital bound to EGFR and potently inhibited the binding of EGF, which prevented the activation of EGFR. This abrogation of EGFR signaling induced the dephosphorylation of receptor for activated C kinase 1 (RACK1) at Tyr^{52}, which then promoted the dephosphorylation of CAR at Thr^{38} by the catalytic core subunit of protein phosphatase 2A. The findings demonstrated that the phenobarbital-induced mechanism of CAR dephosphorylation and activation is mediated through its direct interaction with and inhibition of EGFR.

Introduction

The nuclear receptor CAR [constitutive active androstane receptor; also known as nuclear receptor subfamily 1, group I, member 3 (NR1I3)], a member of the nuclear steroid and thyroid hormone receptor superfamily, is a transcription factor that is indirectly activated by various xenobiotics, such as phenytoin and triclocarban (1, 2), and steroids to promote drug metabolism in the liver. Its localization and therefore its function are regulated by phosphorylation. When it is phosphorylated at Thr^{38}, for example by signaling induced by

*Correspondence: negishi@niehs.nih.gov.

Author contributions

S.M.: design and performance of the experiments and writing of the manuscript; M.S.: ITC analysis; R.M.: experiments with mouse primary hepatocytes; L. Perera: computer simulations and writing of the section on molecular dynamics; L. Pedersen: computer simulations, writing of the section on molecular dynamics, and editing of the manuscript; T.S.: yeast two-hybrid screening; M.N.: project planning and writing of the manuscript.

Competing interests

The authors declare that they have no competing interests.

epidermal growth factor (EGF), CAR is sequestered in the cytoplasm (3–5). Conversely, dephosphorylation of this single residue induces the nuclear translocation of CAR and stimulates its DNA binding capabilities, thereby enabling its transcriptional activity.

Although not a direct ligand of CAR, phenobarbital, a barbiturate widely used to treat epilepsy, induces dephosphorylation of CAR at Thr^{38} and stimulates its transcriptional activity, promoting drug metabolism in the liver (3, 6–8). Since the first report on the metabolic action of phenobarbital nearly 50 years ago (9), this phenomenon has been a fascinating subject of biology and of interest to clinical pharmacology and toxicology. However, the molecular mechanism mediating its physiological action through CAR has remained elusive. CAR mediates not only drug metabolism but also hepatic energy metabolism, cell growth, and cell death (10–13). It is no surprise then that by disrupting metabolic homeostasis, both CAR and phenobarbital are associated with liver injury and liver tumor development and affect drug metabolism in diabetes (10, 11, 14–16). It is thus important to identify the phenobarbital-responsive receptor that mediates the stimulation of CAR to construct and understand the mechanism underlying the biological consequences of its activity.

In this study, we investigated the molecular mechanism of phenobarbital -induced CAR activity relevant to the EGF receptor. We identified the scaffold protein RACK1 (receptor for activated C kinase 1) (17) as a CAR-binding protein. In response to phenobarbital, RACK1 is dephosphorylated and directly activated the protein phosphatase 2A (PP2A) core enzyme (consisting of a catalytic subunit and a scaffolding subunit, herein called PP2Ac), which dephosphorylated CAR at Thr^{38}. In contrast, EGF stimulated phosphorylation of Tyr^{52} RACK1 through epidermal growth factor receptor (EGFR)–mediated activation of the kinase Src. The findings suggest that there is competitive binding and signal transduction between phenobarbital and EGF at the EGF receptor, and thus identify EGFR as a phenobarbital-responsive receptor.

Results

Phenobarbital represses EGF activation of EGFR

The phosphorylation status of CAR and EGFR in response to phenobarbital and EGF was confirmed using whole-cell lysates from mouse primary hepatocytes. In unperturbed cells cultured in normal growth medium, CAR was phosphorylated at Thr^{38}. Whereas treatment with the protein phosphatase inhibitor okadaic acid increased the phosphorylation of CAR at Thr^{38}, treatment with phenobarbital decreased phosphorylation at this site below the detection limits of Western blot analysis (Fig. 1A). As expected, given its inhibition of phosphatase activity, cotreatment with okadaic acid repressed the dephosphorylation induced by phenobarbital. Treatment of cells with EGF increased the phosphorylation of Thr^{38} of CAR and likewise repressed the action of phenobarbital (4 and 5). We therefore hypothesized that phenobarbital may stimulate the dephosphorylation of CAR by antagonizing EGF-induced activation of EGFR. Treatment of mouse primary hepatocytes with EGF induced the phosphorylation of EGFR at Tyr^{845} and Tyr^{1173}; however, subsequent treatment with phenobarbital decreased this EGF-induced phosphorylation at both sites (Fig. 1B and fig. S1). Moreover, pretreatment with phenobarbital substantially suppressed the

ability of EGF to stimulate phosphorylation of EGFR, suggesting that phenobarbital can block the interaction of EGF and EGFR.

RACK1 stimulates CAR dephosphorylation by PP2Ac

The association of RACK1 with phosphorylation-mimicking or nonphosphorylatable mutants of CAR at Thr^{38} was investigated using yeast two -hybrid screens. RACK1 was a cloned protein that preferentially associated with the phosphorylation-mimicking mutant T38D than the nonphosphorylatable mutant T38A (fig. S2), indicating that RACK1 recognizes the phosphorylation signal at Thr^{38} to interact with CAR. Coimmunoprecipitation assays with FLAG-tagged T38D and T38A CAR in Huh7 cells confirmed this finding because RACK1 bound only to the phosphorylation-mimicking mutant (Fig. 2A). In contrast, PP2Ac showed no binding preference (Fig. 2A). These results indicate that RACK1, phosphorylated CAR, and PP2Ac may bind in a complex. RACK1 and PP2A share a common binding region (from residues 140 to 152) within the ligand binding domain (LBD) of CAR (fig. S3, A and B). This binding region is located on the opposite side of a pocket formed with the DNA binding domain (DBD) of CAR that contains Thr^{38} (fig. S3C).

An in vitro dephosphorylation assay was performed with recombinant CAR phosphorylated at Thr^{38} and PP2Ac in the presence or absence of recombinant RACK1. Dephosphorylation of CAR occurred only in the presence of RACK1 (Fig. 2B). Moreover, RACK1 did not stimulate the dephosphorylation of a mutant CAR in which the binding domain was deleted (Fig. 2C). Together, these data suggest that RACK1 and PP2Ac bind to residues 140 to 152 within the LBD of CAR, where PP2Ac dephosphorylates Thr^{38} in the DBD of CAR.

RACK1 is required for CAR de-phosphorylation in hepatocytes

The transcriptional targets of CAR include various genes involved in drug metabolism in the liver. One such gene is *Cyp2b10*, which encodes the mouse homolog of cytochrome P450 2B6, a protein that catalyzes oxidation reactions. Mouse primary hepatocytes were transfected with short hairpin RNA (shRNA) targeting *RACK1*and subsequently treated with either phosphate-buffered saline (PBS) or phenobarbital. Knockdown of *RACK1* significantly attenuated phenobarbital-induced increase in the amount of *Cyp2b10* mRNA (Fig. 3A), indicating that RACK1 was essential in stimulating the transcriptional activity of CAR. Knockdown of *RACK1*also prevented the dephosphorylation of CAR at Thr^{38} (Fig. 3B). Similarly, knockdown of *PP2Ac*with targeted shRNA also prevented the dephosphorylation of CAR at Thr^{38} (Fig. 3C). Together, these data confirm the roles of RACK1 and PP2Ac in the phenobarbital-responsive mechanism promoting the activity of CAR.

Phosphorylation of Tyr^{52} regulates RACK1 activity

We next investigated whether EGF treatment affected the phosphorylation status of RACK1. Immunodetection of endogenous RACK1 in Huh7 cells showed that EGF induced the phosphorylation of RACK1 at Tyr^{52} (Fig. 4A). In Huh7 cells expressing FLAG-tagged wild-type RACK1 or three different tyrosine mutants (Y52F, Y194F, and Y302F), EGF treatment stimulated the phosphorylation of RACK1 only at Tyr^{52} (fig. S4). Furthermore, EGF-

induced phosphorylation of RACK1 abrogated the binding of RACK1 to CAR T38D (Fig. 4B). To further examine the functional effects of phosphorylating this residue, we substituted Tyr^{52} of FLAG -tagged RACK1 with glutamic acid (Y52E) or phenylalanine (Y52F) to create phosphorylation-mimicking and nonphosphorylatable RACK1 mutants, respectively. Only the nonphosphorylatable RACK1 mutant bound to yellow fluorescent protein (YFP)–tagged CAR T38D in transfected Huh7 cells (Fig. 4C). Moreover, the phosphorylation mimic RACK1-Y52E did not stimulate PP2Ac to dephosphorylate Thr^{38} of CAR (Fig. 4D).

Together, these data suggest that RACK1 binds to phosphorylated CAR only when its Tyr^{52} residue is not phosphorylated, and that EGF, by phosphorylating RACK1, directly abolishes this interaction.

The tyrosine kinase Src mediates EGF-induced activation of downstream signal transducers, such as extracellular signal–related kinase (ERK) (18). Src phosphorylates RACK1 at Tyr^{228} and Tyr^{246} (19). In this study, Src appeared to be the enzyme that phosphorylates RACK1 at Tyr^{52}. Src phosphorylated Tyr^{52} of recombinant wild -type RACK1 but not the RACK1 Y52F mutant in an in vitro kinase assay (Fig. 5A). Western blot analysis of liver extracts from mice showed that phenobarbital induced the dephosphorylation of RACK1 at Tyr^{52} in a time -dependent manner (Fig. 5B). Moreover, phenobarbital decreased the phosphorylation of EGFR at Tyr^{845} (Fig. 5C), a site that is phosphorylated by Src in response to EGF (20), suggesting that Src activity may be repressed by phenobarbital. Thus, EGF may stimulate Src kinase to phosphorylate Tyr^{52} of RACK1, thereby blocking the interaction between RACK1, CAR, and PP2Ac; however, phenobarbital represses this mechanism by blocking the EGF-induced activation of EGFR. Tyr^{52} of RACK1 was dephosphorylated by protein tyrosine phosphatase 1B (PTP1B) in an in vitro assay (fig. S5). However, it remains to be examined whether PTP1B is involved in phenobarbital-induced dephosphorylation of RACK1 in hepatocytes in vivo.

Phenobarbital binds to EGFR

Because phenobarbital antagonized EGF activation of EGFR (Fig. 1B) and repressed Src kinase–mediated phosphorylation of RACK1 (Fig. 5B), we next investigated whether phenobarbital directly bound to EGFR. To do this, we incubated a GST-tagged extracellular region of EGFR with biotin-conjugated EGF in the presence of phenobarbital and performed affinity chromatography for purification of EGF-EGFR complex. Phenobarbital reduced the amount of EGF bound to EGFR by more than 60% (Fig. 6A). Performing the assay with immobilized EGFR in reactions containing increasing concentrations of phenobarbital showed that the apparent effective dose of phenobarbital at which it decreased the EGF-EGFR interaction by 50% (the ED_{50}) was about 10 μM (Fig. 6B). Phenobarbital at 10 μM repressed the phosphorylation of EGFR by 17 nM EGF (fig. S6). Furthermore, using isothermal titration calorimetry (ITC), we examined the direct binding of phenobarbital to EGFR and found that phenobarbital bound to EGFR in an endothermic reaction with a dissociation constant (K_d) of about 12 μM (Fig. 6C). These apparent phenobarbital binding affinities appear to be about 1000 times lower than EGF binding to EGFR. ITC analysis

detected five binding sites for phenobarbital in EGFR, although only one K_d value for binding was identified.

We next predicted interaction sites at or near the EGF-binding surface of active or inactive EGFR using docking algorithms. After adopting an optimization scheme that accounts for solvation and dynamics, we performed scoring using the binding energies of phenobarbital to EGFR. The docking model predicted that phenobarbital binds to sites in and near the EGF binding region of EGFR, regardless of its activation state. Eight of the predicted binding positions are shown (tables S1 and S2 and Fig. 6D), the strongest of which are located in site 1 for the active form of EGFR and in site 5 for the inactive form. Sites 1 and 7 exactly overlap, whereas sites 3 and 6 partially overlap. Although outside the direct EGF binding region, site 5 is located in a critical hinge region that controls the motion necessary for switching from the inactive to the active form.

Discussion

Our findings define EGFR as the initial binding site for phenobarbital-induced activation of CAR in the liver. We also characterized RACK1 as the key switch that mediates this activation signal (Fig. 7). RACK1 was phosphorylated at Tyr^{52} by Src kinase in an EGF -dependent manner. Phenobarbital binding to EGFR repressed this Src kinase activity, inducing the dephosphorylation of RACK1 at Tyr^{52}. Phosphorylated residue Tyr^{52} could be dephosphorylated by PTP1B; however, whether this phosphatase, which associates with EGFR (21), dephosphorylates RACK1 in response to phenobarbital treatment requires further investigation. Subsequently, nonphosphorylated RACK1 bound to phosphorylated CAR and PP2Ac, stimulating PP2A to dephosphorylate CAR at Thr^{38}, thereby enabling its activity.

Both the ED_{50} of phenobarbital -mediated repression of EGF binding to EGFR and the K_d value for phenobarbital's binding to EGFR were about 12 μM. Moreover, 10 μM phenobarbital inhibited the activation of EGFR by EGF in mouse primary hepatocytes (which is within the generally observed range for drug–nuclear receptor interactions). Therefore, EGFR appears to be a direct target of phenobarbital, although phenobarbital binding to EGFR at multiple sites appears to differ from those drug-activated nuclear receptors for which one molecule of a given ligand binds to one receptor molecule. The idea that phenobarbital represses EGFR signaling in rat primary hepatocytes has been suggested previously (22). However, in that study, phenobarbital did not inhibit the binding of ^{125}I-labeled EGF to rat primary hepatocytes at 4°C, whereas unlabeled EGF did so effectively, suggesting that phenobarbital may repress EGFR signaling without reducing EGF binding. Although this proposed mechanism remains a possibility, our results support the hypothesis that phenobarbital directly competes with EGF for EGFR. Dynamic simulation of the docking of phenobarbital to a solution model of EGFR based on x-ray crystal structures revealed phenobarbital binding sites that overlap with EGF binding sites. It also predicted that phenobarbital may bind to sites residing in the hinge region that confers a critical conformational change to switch EGFR from an inactive to an active form (23, 24). Therefore, it may be that these multiple bindings collectively compete with EGF binding to repress EGFR activation.

In addition to EGF, other cell signal entities, such as insulin and insulin-like growth factor (IGF), repress phenobarbital's induction of drug metabolism (25, 26). IGF stimulates the phosphorylation of RACK1 at Try^{52} through c-Abl kinase (27). Also, insulin is known to associate EGFR with Src kinase, which results in phosphorylation of Tyr^{845} of EGFR (28). Thus, RACK1 may provide a common regulatory target whereupon signaling induced by various physiological stimuli converge and repress phenobarbital activation of CAR and associated drug metabolism in the liver. Moreover, these membrane receptors provide targets through which drugs and endogenous cell signaling stimuli can cross-talk to regulate CAR activation. In other cell types, RACK1 is involved in the PP2A-mediated dephosphorylation of several other proteins by PP2A, for example, the dephosphorylation of glucose-stimulated inositol-requiring enzyme 1α in pancreatic β cells. RACK1 regulates β_1 integrin –associated PP2A to promote cell migration (29). In addition to the Src kinase pathway, phenobarbital treatment also represses the ERK pathway (5). Because phenobarbital binding to EGFR could simultaneously activate diverse signaling pathways that can affect various cellular functions far beyond CAR activation, it raises the question of how CAR deals with ERK signaling. An intramolecular peptide called XRS (xenobiotic response signal) near the C terminus of CAR interacts with activated ERK and represses the dephosphorylation of Thr^{38} in CAR (5, 30). Thus, XRS appears to constitute a part of the cell signaling mechanism that regulates CAR in response to EGF; whether or not RACK1 is involved in the molecular interaction between ERK and XRS remains to be established.

In conclusion, we identified the molecular mechanism by which phenobarbital indirectly dephosphorylates CAR to induce its transcriptional activity. Although CAR is often referred to as a xenobiotic-sensing nuclear receptor, CAR, in principle, is arguably a cell signaling–regulated nuclear receptor. Drugs such as phenobarbital (and xenobiotics) interact with cell membrane receptors to indirectly activate CAR. These findings provide an initial glimpse into the underlying mechanism, which we can broadly apply to investigate various drug actions through nuclear receptors other than CAR.

Materials and Methods

Cloning RACK1

A human liver complementary DNA (cDNA) library was screened using the DBD of human wild-type CAR, CAR T38A, and CAR T38D as baits and Matchmaker yeast two-hybrid system (Clontech). Through rescreening, *RACK1* was cloned and characterized as a protein that preferentially interacted with the CAR T38D mutant.

Materials

Phenobarbital, antibodies against FLAG M2 agarose, and horseradish peroxidase (HRP)–conjugated FLAG M2 were purchased from Sigma. EGF, okadaic acid, purified active Src kinase, and purified PP2Ac were purchased from Calbiochem. Protease inhibitor cocktail tablets were from Roche. The QuikChange site-directed mutagenesis kit was from Stratagene. Protein A and protein L resins were purchased from Pierce. Antibodies against PP2Ac and RACK1 and mouse normal immunoglobulin M (IgM) were obtained from BD Biosciences. Antibody against actin and HRP-conjugated antibodies against rabbit or mouse

IgG (raised in goat) and normal mouse IgG were purchased from Santa Cruz Biotechnology. Enhanced chemiluminescence reagents and polyvinylidene difluoride (PVDF) membranes were from GE Healthcare. Antibody against CAR was from Perseus Proteomics; antibodies against green fluorescent protein (HRP-conjugated) and purified, active Src kinase were purchased from Abcam. Antibodies against EGFR and phosphorylated EGFR (Tyr^{845} and Tyr^{1173}) were from Cell Signaling Technology. An antibody against the phosphorylated Tyr^{52} of RACK1 was produced in rabbits for this study, using the peptide DETNpYGPQRALRGH (corresponding to residues 48 to 61 of RACK1). The specificity of the antibody was evaluated by enzyme-linked immunosorbent assay with phosphorylated and nonphosphorylated peptides. Antibody against the phosphorylated Thr^{38} of CAR peptide was produced in our previous work (3).

Plasmids and lentiviruses

Human CAR (hCAR) cDNA was previously cloned into pGEX4T-3 (GE Healthcare) to produce GST-CAR fusion proteins, pEYFP-c1 (Clontech) and pCR3 (Invitrogen) (3, 30). A DNA fragment of FLAG tag was placed at the 5′ end of hCAR in pCR3. The full-length RACK1 cDNA was amplified and cloned into pGEX4T-3 and pFLAG-6a (Sigma). Using a QuikChange site-directed mutagenesis kit and appropriately mutated primers, we constructed and confirmed all of the mutants used by nucleotide sequencing. Plasmids were transfected into Huh7 cells with Fugene6 (Roche) according to the manufacturer's instructions. For production of lentiviruses, plasmids that contain shRNAs for PP2A catalytic subunit α and RACK1 (Sigma) were selected for the highest efficiency of knockdown in mouse hematoma-derived Hepa1 cells. These selected plasmids were cotransfected with a lentiviral packaging mix (Sigma) into human embryonic kidney 293T cells [American Type Culture Collection (ATCC)] for 48 hours. The culture medium was collected and centrifuged to remove cell debris and to harvest lentivirus.

Cells

Huh7 cells were maintained in minimum essential medium (Gibco BRL) supplemented with 10% fetal bovine serum (FBS) (Atlanta Biologicals), 2 mM l-glutamine, penicillin (100 U/ml), and streptomycin (100 μg/ml). Mouse primary hepatocytes were isolated from 6-to 8 -week-old C3H/HeNCrIBr male mice (Charles River) using a two-step collagenase perfusion and seeded on 10-cm dishes or six-well plates as described previously (3). One hour after seeding, the culture medium was changed to prewarmed Williams' E medium containing 10% FBS, 1 mM sodium pyruvate, penicillin (100 U/ml), and streptomycin (100 μg/ml).

In vitro dephosphorylation assays

GST-hCAR was phosphorylated in vitro by PKC (Promega) in the presence of adenosine 5′-triphosphate and was purified as previously described (3). Phosphorylated GST-CAR at 1 μM [in 50 mM tris-HCl buffer (pH 8.0) containing 150 mM NaCl] was incubated with 0, 0.5, and 5 μM GST-RACK1 and 0.1 U of PP2Ac for 10 or 30 min at 30°C. The reaction was terminated with SDS–polyacrylamide gel electrophoresis (SDS-PAGE) sample buffer, and lysates were assessed for phosphorylated Thr^{38} by Western blotting.

shRNA transfection

Mouse primary hepatocytes were infected with a 20 MOI (multiplicity of infection) of lentivirus bearing shRNA against RACK1 or lentivirus bearing shRNA against PP2Ac for 24 hours. After being treated with vehicle (PBS) or phenobarbital (2.5 mM) for an additional 2 hours, the primary hepatocytes were extracted in TRIzol for mRNAs or in 50 mM tris-HCl buffer saline (pH 7.6) containing 8 M urea and 1% SDS for proteins.

Immunoprecipitation and Western blot

Huh7 cells were lysed by sonication in a FLAG lysis buffer [tris-HCl (pH 7.6) containing protease inhibitor cocktail, 0.5 mM EDTA, 100 mM NaCl, 1% Triton X-100, 10% glycerol] and centrifuged at 15,000 rpm for 5 min. The resulting supernatant was incubated with the indicated antibody and applied on protein A or protein L resin, which was washed three times with FLAG lysis buffer containing 500 mM NaCl and then added to SDS-PAGE sample buffer. Mouse primary hepatocytes were homogenized in 50 mM tris-HCl buffer saline (pH 7.6) containing 8 M urea and 1% SDS and centrifuged. Proteins were separated by SDS-PAGE and transferred onto a PVDF membrane for Western blot analysis to determine the phosphorylation of Thr^{38} as previously described (3).

Binding assays

Superose 6 gel chromatography assay—The GST-fused extracellular domain of EGFR (containing amino acid residues from 1 to 615) (constructed from a full-length cDNA clone obtained from ATCC) was expressed and purified from *Escherichia coli* BL21(DE3) (Stratagene) with GSH (reduced glutathione)–Sepharose (GE Healthcare). GST-EGFR (3 μg) and biotin-conjugated EGF (10 μg, Invitrogen) were incubated in 100 μl of PBS buffer at room temperature for 10 min, before adding phenobarbital to a final concentration of 100 μM for an additional 10-min incubation. Subsequently, reaction mixtures were chromatographed through a Superose 6 column (10 × 30 cm). Fractions from the first peak were pooled, incubated with GSH-Sepharose for 10 min, and then washed with PBS four times. Biotin-conjugated EGF bound to GST-EGFR on GSH-Sepharose was quantified by HRP-conjugated streptavidin, with 3,3′,5,5″-tetramethybenzidine (TMB) as substrate.

Pull-down assay—GST-EGFR (3 μg) was immobilized on GSH-Sepharose and incubated with biotin-conjugated EGF (10 μg) at room temperature for 10 min in the presence of phenobarbital (0, 1, 10, or 100 μM). Resulting GSH-Sepharose was washed with PBS four times and then subjected to quantification with biotin-conjugated EGF, using HRP-conjugated streptavidin and TMB. ITC measurements were carried out in PBS with an iTC_{200} MicroCalorimeter (GE Healthcare) at 25°C. Substrate solutions containing phenobarbital at 1 mM were injected into a reaction cell containing ~10 to 15 μM protein. Fifty injections of 0.7 μl at 120-s intervals were performed. Data acquisition and analysis were performed with the Origin Scientific Graphing and Analysis software package (OriginLab) and by generating a binding isotherm and best fit using standard Levenberg-Marquardt methods (31).

Docking simulation

Phenobarbital, initially geometrically optimized using Gaussian09-C01 (32) at the B3LYP/cc-pvtz level, was docked to active and inactive conformations of EGF-bound human EGF receptors from x-ray crystal structures(Protein Data Bank ID: 1IVO and 1NQL, respectively) using Autodock (33) and Fred and Hybrid programs (OpenEye Software Inc.). To provide uniform scoring, we also subjected these docked structures to optimization under a Generalized Born (GB) procedure in Amber-12 (34). The raw docked structures were first energy-optimized under the GB scheme [10 K for100 ps and then at 100 K for 1 ns with no constraints on any atom, using the Amber ff03 force field (35)]. The charges of phenobarbital were derived using the CHelpG scheme in Gaussian09 on the optimized structure. Other necessary force field parameters were introduced using the Antechamber module of Amber-12. The top four scoring candidates from the active and inactive sets were fully solvated and subjected to equilibration molecular dynamics runs of 1 ns with 20 kcal/mol constraints on the non-water atoms. The constraints were reduced to 1 kcal/mol, and additional runs (0.5 to 1 ns) were then performed. The final structures were once again energy-minimized. The Coulomb and van der Waals interaction energies between the phenobarbital and EGFR or water were calculated using no cutoff. To establish a reference interaction energy for phenobarbital in water, we performed an all-atom Amber trajectory calculation for a system containing a phenobarbital dissolved in a box of 10,375 water molecules. After following a standard equilibration protocol, a 25-ns production run with a constant number of molecules and constant volume and temperature was carried out. Interaction energies and their components were then calculated from the 15 structures of the phenobarbital and water system obtained for the last 15 ns at 1-ns intervals.

Supplementary Material

Refer to Web version on PubMed Central for supplementary material.

Acknowledgments

We thank the members of the Pharmacogenetics section, in particular M. Osabe for valuable discussion. We also thank D. Armstrong for his critical reading of the manuscript.

Funding

This research was supported by the Intramural Research Program of the NIH (HL-06350) and the National Institute of Environmental Health Sciences (Z01ES1005-01).

References

1. Jackson JP, Ferguson SS, Moore R, Negishi M, Goldstein JA. The constitutive active/androstane receptor regulates phenytoin induction of Cyp2c29. Mol Pharmacol. 2004; 65:1397–1404. [PubMed: 15155833]
2. Yueh MF, Li T, Evans RM, Hammock B, Tukey RH. Triclocarban mediates induction of xenobiotic metabolism through activation of the constitutive androstane receptor and the estrogen receptor alpha. PLoS One. 2012; 7:e37705. [PubMed: 22761658]
3. Mutoh S, Osabe M, Inoue K, Moore R, Pedersen L, Perera L, Rebolloso Y, Sueyoshi T, Negishi M. Dephosphorylation of threonine 38 is required for nuclear translocation and activation of human xenobiotic receptor CAR (NR1I3). J Biol Chem. 2009; 284:34785–34792. [PubMed: 19858220]

4. Koike C, Moore R, Negishi M. Extracellular signal-regulated kinase is an endogenous signal retaining the nuclear constitutive active/androstane receptor (CAR) in the cytoplasm of mouse primary hepatocytes. Mol Pharmacol. 2007; 71:1217–1221. [PubMed: 17314319]
5. Osabe M, Negishi M. Active ERK1/2 protein interacts with the phosphorylated nuclear constitutive active/androstane receptor (CAR; NR1I3), repressing dephosphorylation and sequestering CAR in the cytoplasm. J Biol Chem. 2011; 286:35763–35679. [PubMed: 21873423]
6. Honkakoski P, Zelko I, Sueyoshi T, Negishi M. The nuclear orphan receptor CARretinoid X receptor heterodimer activates the phenobarbital-responsive enhancer module of the CYP2B gene. Mol Cell Biol. 1998; 18:5652–5658. [PubMed: 9742082]
7. Sueyoshi T, Kawamoto T, Zelko I, Honkakoski P, Negishi M. The repressed nuclear receptor CAR responds to phenobarbital in activating the human CYP2B6 gene. J Biol Chem. 1999; 274:6043–6046. [PubMed: 10037683]
8. Kawamoto T, Sueyoshi T, Zelko I, Moore R, Washburn K, Negishi M. Phenobarbital responsive nuclear translocation of the receptor CAR in induction of the CYP2B gene. Mol Cell Biol. 1999; 19:6318–6322. [PubMed: 10454578]
9. Remmer H, Merker HJ. Drug-induced changes in the liver endoplasmic reticulum: Association with drug-metabolizing enzymes. Science. 1963; 142:1657–1658. [PubMed: 14075694]
10. Wada T, Gao J, Xie W. PXR and CAR in energy metabolism. Trends Endocrinol Metab. 2009; 20:273–279. [PubMed: 19595610]
11. Kodama S, Koike C, Negishi M, Yamamoto Y. Nuclear receptors CAR and PXR cross talk with FOXO1 to regulate genes that encode drug-metabolizing and gluconeogenic enzymes. Mol Cell Biol. 2004; 24:7931–7940. [PubMed: 15340055]
12. Dong B, Saha PK, Huang W, Chen W, Abu-Elheiga LA, Wakil SJ, Stevens RD, Ilkayeva O, Newgard CB, Chan L, Moore DD. Activation of nuclear receptor CAR ameliorates diabetes and fatty liver disease. Proc Natl Acad Sci USA. 2009; 106:18831–18836. [PubMed: 19850873]
13. Yamamoto Y, Moore R, Flavell RA, Lu B, Negishi M. Nuclear receptor CAR represses TNFa-induced cell death by interacting with the anti-apoptotic GADD45B. PLoS One. 2010; 5:e10121. [PubMed: 20404936]
14. Kakizaki S, Yamazaki Y, Takizawa D, Negishi M. New insights on the xenobiotic-sensing nuclear receptors in liver diseases: CAR and PXR. Curr Drug Metab. 2008; 9:614–621. [PubMed: 18781913]
15. Huang W, Zhang J, Washington M, Liu J, Parant JM, Lozano G, Moore DD. Xenobiotic stress induces hepatomegaly and liver tumors via the nuclear receptor constitutive androstane receptor. Mol Endocrinol. 2005; 19:1646–1653. [PubMed: 15831521]
16. Yamamoto Y, Moore R, Goldsworthy TL, Negishi M, Maronpot RR. The orphan nuclear receptor constitutive active/androstane receptor is essential for liver tumor promotion by phenobarbital in mice. Cancer Res. 2004; 64:7197–7200. [PubMed: 15492232]
17. McCahill A, Warwicker J, Bolger GB, Houslay MD, Yarwood SJ. The RACK1 scaffold protein: A dynamic cog in cell response mechanisms. Mol Pharmacol. 2002; 62:1261–1273. [PubMed: 12435793]
18. Tice DA, Biscardi JS, Nickles AL, Parsons SJ. Mechanism of biological synergy between cellular Src and epidermal growth factor receptor. Proc Natl Acad Sci USA. 1999; 96:1415–1420. [PubMed: 9990038]
19. Chang BY, Harte RA, Cartwright CA. RACK1: A novel substrate for the Src protein-tyrosine kinase. Oncogene. 2002; 21:7619–7629. [PubMed: 12400005]
20. Biscardi JS, Maa MC, Tice DA, Cox ME, Leu TH, Parsons SJ. c-Src-mediated phosphorylation of the epidermal growth factor receptor on Tyr845 and Tyr1101 is associated with modulation of receptor function. J Biol Chem. 1999; 274:8335–8343. [PubMed: 10075741]
21. Liu F, Chernoff J. Protein tyrosine phosphatase 1B interacts with and is tyrosine phosphorylated by the epidermal growth factor receptor. Biochem J. 1997; 327:139–145. [PubMed: 9355745]
22. Meyer SA, Gibbs TA, Jirtle RL. Independent mechanisms for tumor promoters phenobarbital and 12-O-tetradcanoylphorbol-13-acetate in reduction of epidermal growth factor binding by rat hepatocytes. Cancer Res. 1989; 49:5907–5912. [PubMed: 2790804]

23. Ogiso H, Ishitani R, Nureki O, Fukai S, Yamanaka M, Kim JH, Saito K, Sakamoto A, Inoue M, Shirouzu M, Yokoyama S. Crystal structure of the complex of human epidermal growth factor and receptor extracellular domains. Cell. 2002; 110:775–787. [PubMed: 12297050]
24. Ferguson KM, Berger MB, Mendrola JM, Cho HS, Leahy DJ, Lemmon MA. EGF activates its receptor by removing interactions that autoinhibit ectodomain dimerization. Mol Cell. 2003; 11:507–517. [PubMed: 12620237]
25. Yoshida Y, Kimura N, Oda H, Kakinuma K. Insulin suppresses the induction of the CYP2B1 and CYP2B2 gene expression by phenobarbital in adult rat culture hepatocytes. Biochem Biophys Res Commun. 1996; 229:182–188. [PubMed: 8954103]
26. Li L, Sinz MW, Zimmermann K, Wang H. An insulin-like growth factor 1 receptor inhibitor induces CYP3A4 expression through a pregnane X receptor-independent, noncanonical constitutive androstane receptor-related mechanism. J Pharmacol Exp Ther. 2012; 340:688–697. [PubMed: 22171088]
27. Kiely PA, Baillie GS, Barrett R, Buckley DA, Adams DR, Houslay MD, O'Connor R. Phosphorylation of RACK1 on tyrosine 52 by c-Abl is required for insulin-like growth factor I-mediated regulation of focal adhesion kinase. J Biol Chem. 2009; 284:20263–20274. [PubMed: 19423701]
28. Reinehr R, Sommerfeld A, Häusssinger D. Insulin induces swelling-dependent activation of the epidermal growth factor receptor in rat liver. J Biol Chem. 2010; 285:25904–25912. [PubMed: 20571033]
29. Qiu Y, Mao T, Zhang Y, Shao M, You J, Ding Q, Chen Y, Wu D, Xie D, Lin X, Gao X, Kaufman RJ, Li W, Liu Y. A crucial role for RACK1 in the regulation of glucose-stimulated IRE1a activation in pancreatic b cells. Sci Signal. 2010; 3:ra7. [PubMed: 20103773]
30. Zelko I, Sueyoshi T, Kawamoto T, Moore R, Negishi M. The peptide near the C terminus regulates receptor CAR nuclear translocation induced by xenochemicals in mouse liver. Mol Cell Biol. 2001; 21:2838–2846. [PubMed: 11283262]
31. Press, WH., Flannery, BP., Teukolsky, SA., Vetterling, WT. Numerical Recipes in FORTRAN: The Art of Scientific Computing. Cambridge University Press; Cambridge: 1989.
32. Frisch, MJ., Trucks, GW., Schlegel, HB., Scuseria, GE., Robb, MA., Cheeseman, JR., Scalmani, G., Barone, V., Mennucci, B., Petersson, GA., Nakatsuji, H., Caricato, M., Li, X., Hratchian, HP., Izmaylov, AF., Bloino, J., Zheng, G., Sonnenberg, JL., Hada, M., Ehara, M., Toyota, K., Fukuda, R., Hasegawa, J., Ishida, M., Nakajima, T., Honda, Y., Kitao, O., Nakai, H., Vreven, T., Montgomery, JA., Jr, Peralta, JE., Ogliaro, F., Bearpark, M., Heyd, JJ., Brothers, E., Kudin, KN., Staroverov, VN., Kobayashi, R., Normand, J., Raghavachari, K., Rendell, A., Burant, JC., Iyengar, SS., Tomasi, J., Cossi, M., Rega, N., Millam, JM., Klene, M., Knox, JE., Cross, JB., Bakken, V., Adamo, C., Jaramillo, J., Gomperts, R., Stratmann, RE., Yazyev, O., Austin, AJ., Cammi, R., Pomelli, C., Ochterski, JW., Martin, RL., Morokuma, K., Zakrzewski, VG., Voth, GA., Salvador, P., Dannenberg, JJ., Dapprich, S., Daniels, AD., Farkas, Ö., Foresman, JB., Ortiz, JV., Cioslowski, J., Fox, DJ. Gaussian 09, Revision C.1. Gaussian Inc; Wallingford, CT: 2009.
33. Morris GM, Huey R, Lindstrom W, Sanner MF, Belew RK, Goodsell DS, Olson AJ. Autodock4 and AutoDockTools4: Automated docking with selective receptor flexibility. J Comput Chem. 2009; 30:2785–2791. [PubMed: 19399780]
34. Case, DA., Darden, TA., Cheatham, TE., III, Simmerling, CL., Wang, J., Duke, RE., Luo, R., Walker, RC., Zhang, W., Merz, KM., Roberts, B., Hayik, S., Roitberg, A., Seabra, G., Swails, J., Götz, AW., Kolossváry, I., Wong, KF., Paesani, F., Vanicek, J., Wolf, RM., Liu, J., Wu, X., Brozell, SR., Steinbrecher, T., Gohlke, H., Cai, Q., Ye, X., Wang, J., Hsieh, M-J., Cui, G., Roe, DR., Mathews, DH., Seetin, MG., Salomon-Ferrer, R., Sagui, C., Babin, V., Luchko, T., Gusarov, S., Kovalenko, A., Kollman, PA. AMBER 12. University of California; San Francisco: 2012.
35. Duan Y, Wu C, Chowdhury S, Lee MC, Xiong G, Zhang W, Yang R, Cieplak P, Luo R, Lee T, Caldwell J, Wang J, Kollman P. A point-charge force field for molecular mechanics simulations of proteins based on condensed-phase quantum mechanical calculations. J Comput Chem. 2003; 24:1999–2012. [PubMed: 14531054]

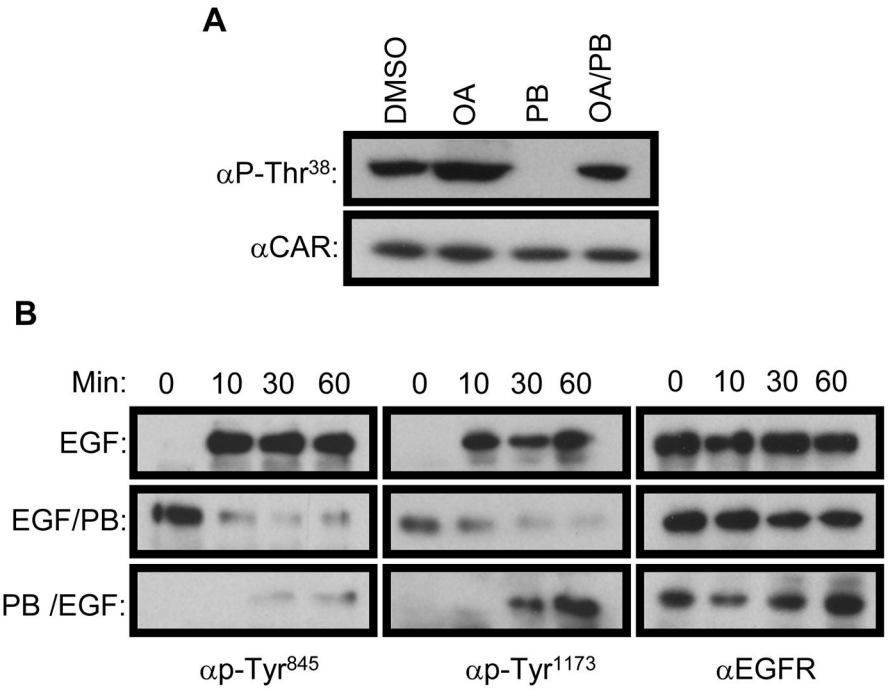

Fig. 1. Phenobarbital antagonizes EGF-induced activation of EGFR

(**A**) Western blot analysis of mouse primary hepatocyte cell extracts treated with 10 nM okadaic acid (OA), 2.5 mM phenobarbital (PB), or both for 2 hours, detecting the phosphorylation of CAR at Thr^{38}. Data shown are representative of three experiments. (**B**) Phenobarbital antagonizes EGF to repress phosphorylation of EGF. Western blot analysis detecting phosphorylated EGFR at Tyr^{845} or Tyr^{1173} in cell extracts from mouse primary hepatocytes treated with EGF (100 μg/ml) for the time indicated, alone (top) or 30 min before (middle) or after (bottom) phenobarbital (2.5 mM) treatment. Data shown are representative of three experiments.

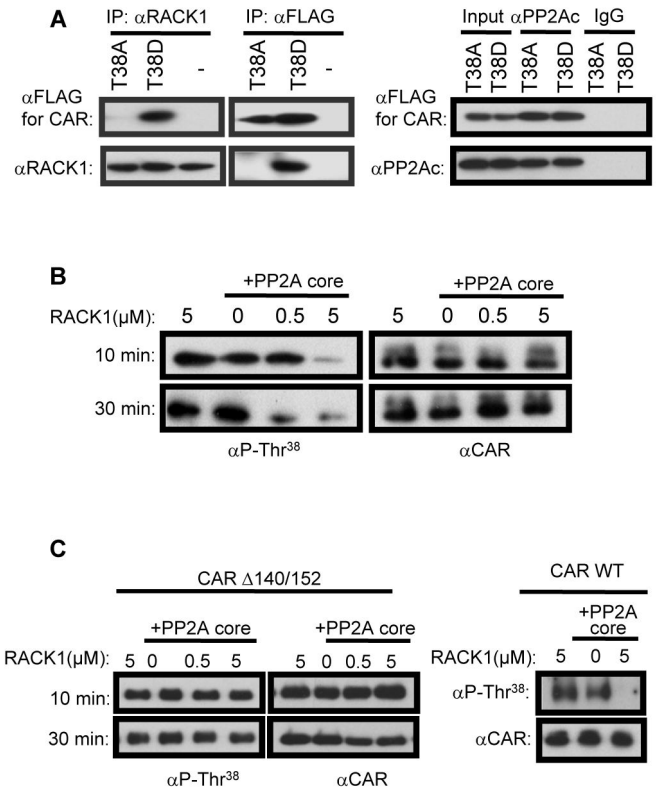

Fig. 2. Phosphorylated CAR interacts with RACK1

(**A**) Immunoprecipitation of RACK1 (left) or PP2Ac (right) and Western blot analysis in Huh7 cells transfected with FLAG-tagged mutant CAR (nonphosphorylatable T38A or phosphorylation mimic T38D). (**B**and **C**) Western blot analysis assessing the in vitro dephosphorylation of wild-type (WT) glutathione *S*-transferase (GST)–tagged CAR (B) or a GST-tagged Δ140/152 CAR mutant (C) at Thr^{38} [phosphorylated by protein kinase C (PKC)] in the presence of purified PP2Ac and recombinant GST -RACK1 (0, 0.5, and 5 μM; 30°C for the indicated times). In (C), dephosphorylation of the WT CAR (right) at 30 min is shown for direct comparison. Data shown are representative of three experiments.

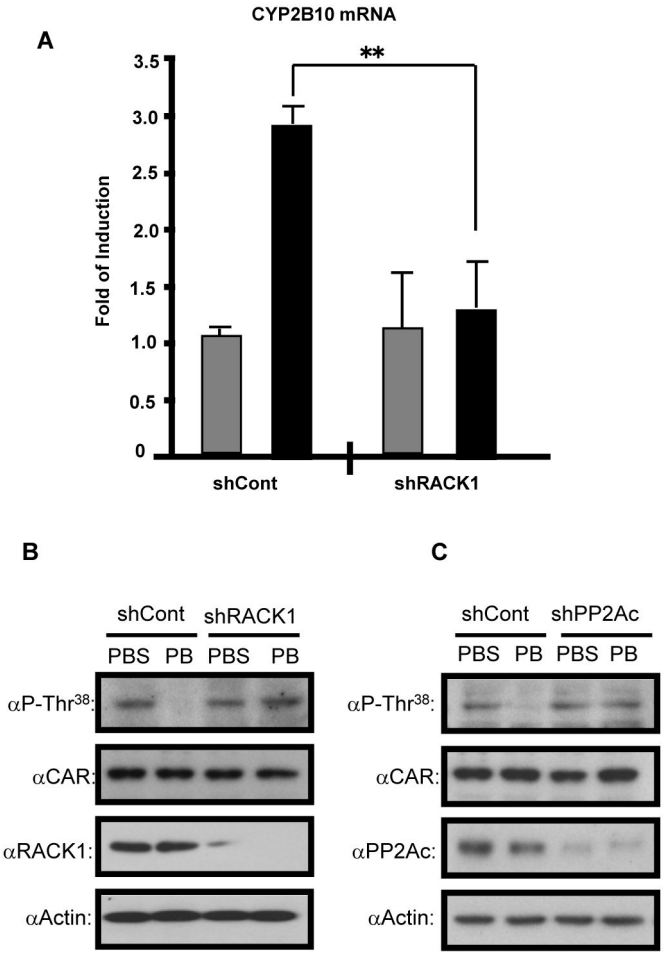

Fig. 3. RACK1 is essential in phenobarbital-induced dephosphorylation of CAR

(**A**) Abundance of *Cyp2b10* mRNA in mouse primary hepatocytes transfected with either control (shCont) or RACK1-specific (shRACK1) shRNA and treated with either PBS or 2.5 mM phenobarbital (black bars). Data are presented as means ± SD of the fold change from PBS-treated control shRNA–transfected cells in X experiments. ** P= 0.0057, Student's t test. (**B**and **C**) Western blot analysis detecting the phosphorylation of CAR at Thr^{38} in response to phenobarbital (PB, 2.5 mM) in either (B) RACK1-depleted or (C) PP2Ac-depleted mouse primary hepatocytes compared with control cells. Data shown are representative of three experiments.

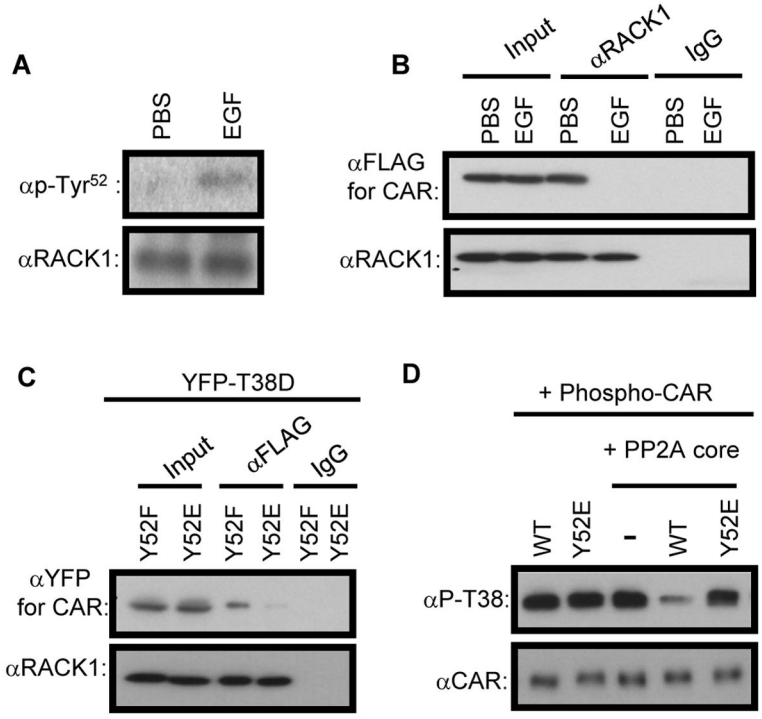

Fig. 4. RACK1 function is regulated by phosphorylation at Tyr^{52}

(**A**) Huh7 cells were treated with EGF (10 ng/ml) or PBS for 30 min, and whole-cell extracts were analyzed by Western blot to assess the phosphorylation of RACK1 at Tyr^{52}. Data shown are representative of three experiments. (**B**) Immunoprecipitation of RACK1 and Western blot analysis detecting RACK1 and CAR were performed in whole-cell extracts of Huh7 cells transfected with FLAG-tagged CAR T38D and treated with EGF (10 ng/ml) or PBS for 30 min. Data shown are representative of three experiments. (**C**) Immunoprecipitation of the FLAG tag and Western blot analysis assessing the abundance of YFP-tagged CAR T38D and FLAG-tagged mutant RACK1 (Y52F or Y52E) in transfected Huh7 cells. (**D**) The effect of WT or mutant RACK1 (Y52E) on the ability of the PP2A core catalytic enzyme to dephosphorylate CAR at Thr^{38} was assessed in vitro. Data shown are representative of three experiments.

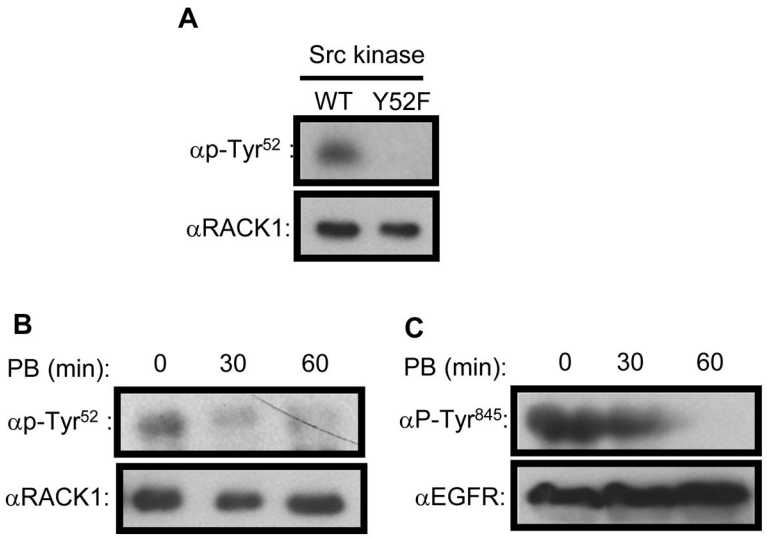

Fig. 5. Phenobarbital represses Src kinase–mediated phosphorylation of RACK1 at Tyr^{52}

(**A**) The phosphorylation of RACK1 at Tyr^{52} was assessed by a kinase assay using purified Src and either WT or mutant RACK1 (Y52F). Data shown are representative of three experiments. (**B**) Phenobarbital (PB, 2.5 mM) was intraperitoneally administered to mice, and Western blot analysis was performed at the indicated times on whole mouse liver extracts. Data shown are representative of three experiments. (**C**) Western blot analysis of the same whole liver extracts used in (B) assessed the phosphorylation of EGFR at Tyr^{845}. Data shown are representative of three experiments.

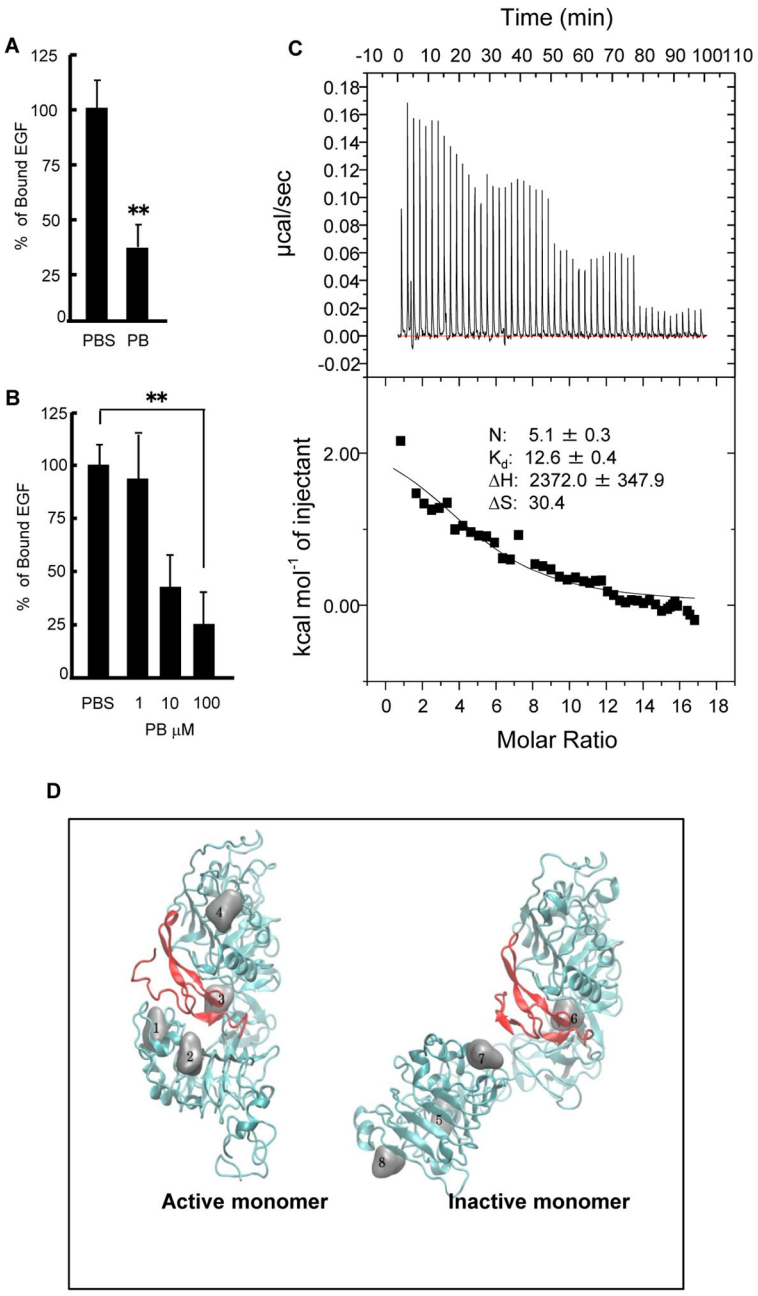

Fig. 6. Phenobarbital competes with EGF to bind EGFR

(**A**) Binding between a GST-tagged extracellular domain of EGFR and biotin-conjugated EGF incubated with and without phenobarbital (PB, 100 μM) for 30 min was assessed by gel chromatography. Data are means ± SD from three independent experiments. ** $P < 0.01$, Student's t test. (**B**) GST-EGFR was immobilized onto beads and incubated with biotin-conjugated EGF in the presence of phenobarbital for 10 min. The amount of bound EGF in the absence of phenobarbital was assumed as 100%. Data are means ± SD from three independent experiments. ** $P < 0.01$, Student's t test. (**C**) ITC assessed the biomolecular interactions between phenobarbital and EGFR [N(number of sites), ΔH (cal/mol), ΔS (cal

mol^{-1} deg^{-1}), and K (binding constant in M $^{-1}$), from which K (M $^{-1}$) is then converted to K_d (μM)]. Data are representative of four independent experiments. (**D**) Eight sites most predicted by docking algorithms where phenobarbital might bind EGFR, either in active state (left) or inactive state (right). The binding location of EGF in each structure is shown using the ribbon representation (in red). The two forms are oriented such that domain I (residues 5 to 150) of EGFR is aligned.

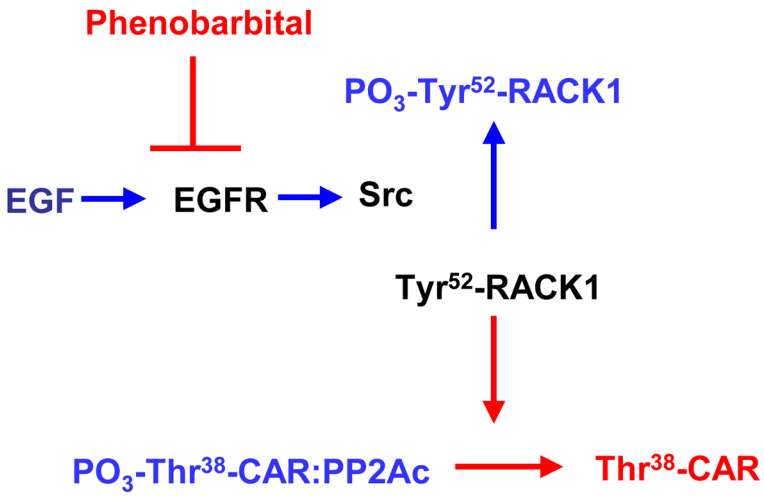

Fig. 7. Phenobarbital directly disrupts EGFR signaling to elicit activation of CAR

A schematic representation of the cell signaling that regulates the activation of CAR is shown. Phenobarbital-induced signaling is shown in red, whereas EGF-mediated signaling is in blue. EGF activates EGFR, which induces Src kinase to phosphorylate RACK1, thereby preventing its interaction with PP2A and CAR. Through competitive binding, phenobarbital blocks the EGF-EGFR interaction, thereby enabling an unphosphorylated RACK1 to interact with PP2A and CAR. Dephosphorylated CAR then translocates to the nucleus where it stimulates the transcription of target genes.